Generator-Coordinate Spectrum of ^{20}Ne

S. B. Khadkikar and D. R. Kulkarni

Physical Research Laboratory, Navrangpura, Ahmedabad 9, India

(Received 6 March 1972; revised manuscript received 24 May 1972)

The generator-coordinate method based on projection from constrained Hartree-Fock states is applied to obtain the $T = 0$ energy levels of ^{20}Ne. The results obtained with the strength of the external quadrupole field as a generator coordinate compare very well with those of exact shell-model calculations.

INTRODUCTION

After the established success of the projected Hartree-Fock (PHF) method to obtain the ground-state bands of nuclei,[1] it is natural to look for a generalization based on this method to obtain higher bands of levels in the nuclear spectra. The validity of such a generalization has to be assessed by comparison with exact shell-model calculations. The aim of the present note is to show that the generator-coordinate[2] calculations with constrained axial Hartree-Fock (HF) states as a basis do provide such a generalization which is simpler and computationally less involved than the alternative formalism of projecting the states from particle-hole excited intrinisic states.[3] Such calculations may also give some insight into the physical nature of the excited states in shell-model spectra.

It may be noted that the generator-coordinate (GC) calculations with Nilsson states as a basis is able to explain[4] the ground-state band of ^{20}Ne. However, it is well known that the PHF method is equally successful and much simpler. Hence one would look for the natural unification of the GC and PHF methods by using constrained HF solutions in projection formalism.

METHOD OF CALCULATIONS

We minimize free energy $E = \langle \phi_\lambda | H - \lambda Q_0^2 | \phi_\lambda \rangle$ in the HF procedure to obtain the state ϕ_λ for the nucleus ^{20}Ne. Then we solve the Hill-Wheeler integral equations;

$$\int F(\lambda')[H^J(\lambda, \lambda') - E^J I^J(\lambda, \lambda')] \, d\lambda' = 0,$$

where

$$H^J(\lambda, \lambda') = \langle \phi_\lambda | HP_{00}^J | \phi_{\lambda'} \rangle,$$

$$I^J(\lambda, \lambda') = \langle \phi_\lambda | P_{00}^J | \phi_{\lambda'} \rangle,$$

and P_{00}^J is the well-known projection operator.[1] The constrained HF solutions are obtained by picking out that branch of the solution which is gener-

ated, as smoothly as possible, out of the lowest prolate HF solution. This is achieved by using the HF solution ϕ_λ as the starting point for the iteration of the solution $\phi_{\lambda+d\lambda}$ where $d\lambda$ is a small increment in the strength of the external quadrupole field. These calculations enable us to plot the graph of free energy (E) vs the quadrupole moment $\langle Q_0^2 \rangle$ as shown in the Fig. 1. It may be noted that the curve is not continuous but sharply divided into two distinct and separate branches, one corresponding to the prolate solutions and the other to the oblate solutions. This feature has already been observed by Bassichis and Wilets[5,6] and Giraud, LeTourneux, and Wong[7] independently for the case of ^{20}Ne. In the region of the discontinuity the HF solutions are unstable and therefore one has to use different iterative techniques to obtain the intermediate points. Giraud, LeTourneux, and Wong have tried to obtain the intermediate points by using what is called "stabilization procedure." This procedure has given rise to multivaluedness in the energy kernels with respect to the quadrupole moment $\langle Q_0^2 \rangle$ as shown schematically in the Fig. 1. On the other hand Bassichis and Wilets[6] could obtain the continuous single-value curve connecting the two branches by adopting a different iterative method as shown schematically in the Fig. 1. Thus, a unique way of connecting the two branches does not exist. We have also plotted the curves of the energy E vs λ and the quadrupole moment $\langle Q_0^2 \rangle$ vs λ as shown in the Fig. 2. The curves indicate the response of the ^{20}Ne HF solution to the strength of the external quadrupole field. The response curves are characterized by a single discontinuity at $\lambda = 0.79$. The existence of this discontinuity does not affect the integrability of the kernels in the Hill-Wheeler integral equation. This encourages us to proceed with the generator coordinate calculations using λ as the generator coordinate. However, the region of the discontinuity if joined by using, for example, the iterative procedure of Bassichis and Wilets[6] leads to multivaluedness with respect to λ also. It would be necessary to incorporate the
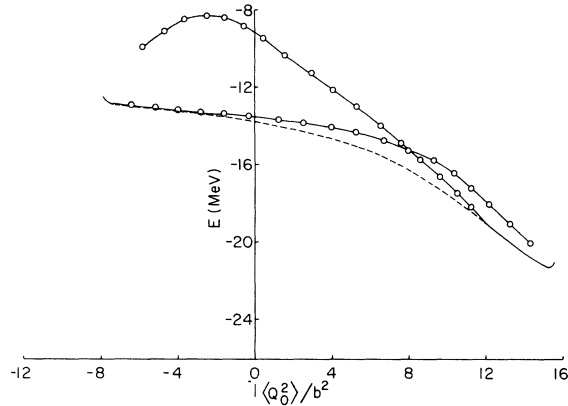
FIG. 1. The variation of HF energy E with the quadrupole moment $\langle Q_0^2\rangle$ (solid-line curve). The dashed-line curve would be the curve connecting the two branches using the method of Bassichis and Wilets and the circled-line curves are those obtained by Giraud, LeTourneux, and Wong, both being shown schematically.

branch sequence as an additional label for the generator coordinate in the case of multivalued kernels to solve the Hill-Wheeler integral equations. However, since one obtains different results for this part of the multivalued kernels using different methods[6,7] we prefer to stick to the kernels obtained in a simple iterative procedure leading to stable solutions. It is gratifying to note that the results of our calculations indicate that the points in the discontinuous region are not necessary for the description of the excited states below 18 MeV in the ^{20}Ne spectrum.

The curves of the energy E vs λ and quadrupole moment $\langle Q_0^2\rangle$ vs λ (Fig. 2) are quite flat owing to the stiffness of the HF solution around prolate as well as oblate deformations. Hence we can approximate the Hill-Wheeler integral equation by
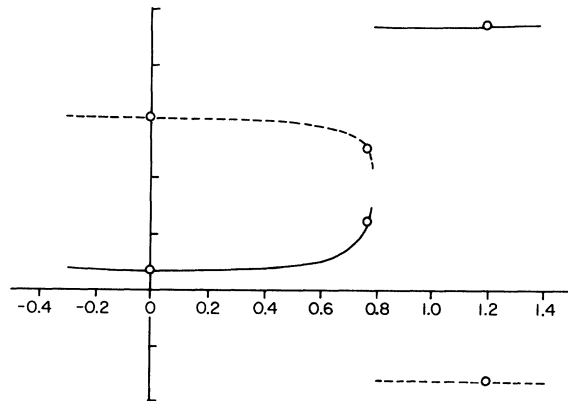
TABLE I. $k = \frac{1}{2}$, orbitals of the three constrained HF solutions for ^{20}Ne with the corresponding HF energy and quadrupole moments. b, the harmonic-oscillator constant is equal to 1.65 fm.

λb^2 (MeV)	$E(\lambda)$ (MeV)	$d_{5/2\ 1/2}$	$s_{1/2\ 1/2}$	$d_{3/2\ 1/2}$	$\langle Q_0^2\rangle/b^2$
0.0	−21.23	0.7703	−0.4985	−0.3976	15.45
0.77	−19.54	0.8745	−0.2563	−0.4118	12.69
1.20	−12.57	0.4870	0.8361	−0.2526	−7.80

making the coordinate λ discrete as follows:

$$\sum_m (E^J_{n,m} - E^J I^J_{n,m}) f_m = 0.$$

It is enough to take few points with sufficiently different deformations as otherwise the Hilbert space $\{\phi^J_\lambda\}$ is overcomplete. We have given the single-particle orbits in the case of ^{20}Ne for the three points which have been used in our calculations in Table I.

We have employed the effective-interaction matrix elements derived by Kuo[8] from the Hamada-Johnston potential, renormalized for the $1d$-$2s$ configuration space used in these calculations along with the experimental single-particle energies of ^{17}O. We have also calculated the ^{20}Ne spectrum by diagonalizing the above Hamiltonian

FIG. 2. The variation of Hartree-Fock energy E (solid-line curve) and that of quadrupole moment $\langle Q_0^2\rangle$ (dashed-line curve) with λ. Both the curves are drawn in arbitrary units. The circled points (see Table I) are used in GC calculations.
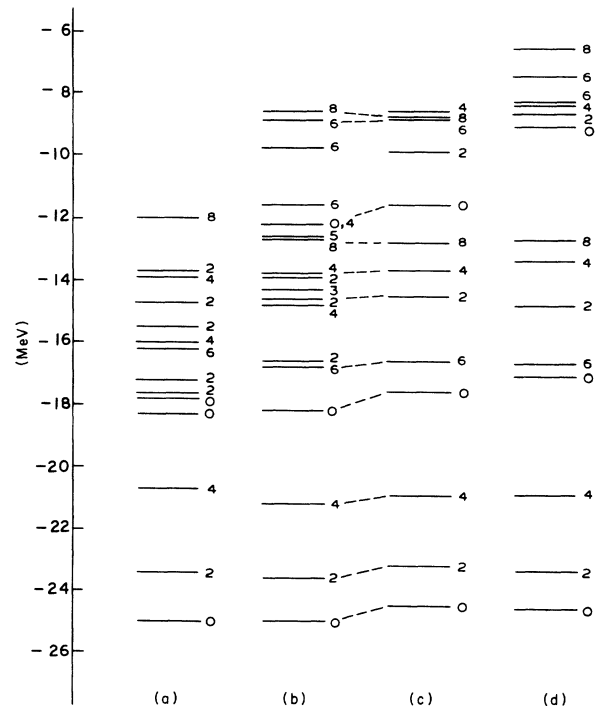
FIG. 3. Positive-parity $T = 0$ energy levels in the ^{20}Ne spectrum: (a) the experimental; (b) the shell model; (c) the GC method; (d) the projected one particle-one hole as explained in the text.

in the space of good angular momentum states projected from the prolate HF state as well as the $K = 0$, $T = 0$ states obtained by one-particle-one-hole (1p-1h) excitations, taking proper care of nonorthonormality. The results of the GC calculations along with the above results are compared with the results of the exact shell-model[9] calculations for $T = 0$ states in Fig. 3. We have plotted the energies in absolute scale to facilitate a meaningful comparison of different methods.

RESULTS AND DISCUSSIONS

In general the agreement between the GC spectrum and the corresponding $T = 0$ levels in the shell-model spectrum is quite good. We have been able to identify 11 levels in shell-model spectrum which are generated in these axially symmetric GC calculations. For the highest levels in the GC spectrum with angular momentum 2 and 4 we do not have the corresponding results of exact shell-model calculations for comparison; there are several levels in the shell-model spectrum at excitation of 8–10 MeV, which are not obtained in axial GC calculations. However, as the $K = 2$, 1p-1h excited band is around the same region of excitation, we expect that these states also could be generated with a nonaxial GC calculation. For example, the band of levels starting with the 2^+ at –16.8 MeV is presumably nonaxial. Otherwise the GC results are consistently better in agreement with the exact shell-model results than those obtained through 1p-1h projection calcula-

tion. It is known that the shape mixing with higher HF solution is required to improve the agreement[10] between the particle-hole spectra and the shell-model results.

We have shown that the constrained HF solutions with axial symmetry can be chosen as a basis for the GC calculations, and give an excellent agreement with a major part of the shell-model spectrum below 18 MeV excitation even though we have omitted points in the unstable region. It may be possible to reproduce all the $T = 0$ shell-model levels below 18 MeV excitation through addition of the nonaxial deformations in the GC method rather than extending the kernels to the unstable region. At the same time it will be of great interest to study the correlations between the generation of states and the transition probabilities. In the experimental spectrum (Fig. 3), however, there are many levels which presumably arise from core excitations. The results of the present calculations encourage us to perform the GC calculations taking into account all the nucleons in the nucleus and a suitably large Hilbert space. Such calculations, though lengthy, are feasible.[11] It would also be interesting to study the connection between the important shape-mixing effects present in the neutron excess nuclei[12] and corresponding GC calculations. Attempts in this direction are in progress.

[1]G. Ripka, in *Advances in Nuclear Physics,* edited by M. Baranger and E. Vogt (Plenum, New York, 1968), Vol. I; C. S. Warke and M. R. Gunye, Phys. Rev. 155, 1048 (1969); M. R. Gunye and C. S. Warke, Phys. Rev. 156, 1087 (1969).

[2]D. L. Hill and J. A. Wheeler, Phys. Rev. 89, 1102 (1953).

[3]M. H. Macfarlane and A. P. Shukla, Phys. Letters 35B, 11 (1971).

[4]M. V. Mihailovic, E. Kujawski, and J. Lesjak, Nucl. Phys. A161, 252 (1971).

[5]W. H. Bassichis and L. Wilets, Phys. Rev. Letters 22, 799 (1969).

[6]W. H. Bassichis and L. Wilets, Phys. Rev. Letters 27, 1451 (1971).

[7]B. Giraud, J. LeTourneux, and S. K. M. Wong, Phys. Letters 32B, 23 (1970). Also see the invited talk by J. LeTourneux, in *Proceedings of the International Conference on Properties of Nuclear States, Montreal, Canada, 1969,* edited by M. Harvey *et al.* (Presses de l'Université de Montréal, Montréal, Canada, 1969), p. 599.

[8]T. T. S. Kuo, Nucl. Phys. A103, 71 (1967).

[9]J. B. McGrory, private communication.

[10]S. N. Tewari, Phys. Letters 29B, 5 (1969).

[11]M. R. Gunye and S. B. Khadkikar, Phys. Rev. Letters 24, 910 (1970).

[12]S. B. Khadkikar, S. C. K. Nair, and S. P. Pandya, Phys. Letters 36B, 290 (1971).